AFRL-AFOSR-UK-TR-2014-0027

Multi-object filtering for space situational awareness

Daniel Clark
Emmanuel Delande
Carolin Frueh

HERIOT-WATT UNIVERSITY
RICCARTON
EDINBURGH, EH14 4AS
UNITED KINGDOM

EOARD Grant 13-3030

Report Date: June 2014

Final Report from 28 February 2013 to 31 March 2014

Air Force Research Laboratory
Air Force Office of Scientific Research
European Office of Aerospace Research and Development
Unit 4515, APO AE 09421-4515

REPORT DOCUMENTATION PAGE

Form Approved OMB No. 0704-0188

1. REPORT DATE *(DD-MM-YYYY)*	2. REPORT TYPE	3. DATES COVERED *(From – To)*
11 June 2014	Final Report	28 February 2013 – 31 March 2014

4. TITLE AND SUBTITLE

Multi-object filtering for space situational awareness

5a. CONTRACT NUMBER

FA8655-13-1-3030

5b. GRANT NUMBER

Grant 13-3030

5c. PROGRAM ELEMENT NUMBER

61102F

6. AUTHOR(S)

Daniel Clark
Emmanuel Delande
Carolin Frueh

5d. PROJECT NUMBER

5d. TASK NUMBER

5e. WORK UNIT NUMBER

7. PERFORMING ORGANIZATION NAME(S) AND ADDRESS(ES)

HERIOT-WATT UNIVERSITY
RICCARTON
EDINBURGH, EH14 4AS
UNITED KINGDOM

8. PERFORMING ORGANIZATION REPORT NUMBER

N/A

9. SPONSORING/MONITORING AGENCY NAME(S) AND ADDRESS(ES)

EOARD
Unit 4515
APO AE 09421-4515

10. SPONSOR/MONITOR'S ACRONYM(S)

AFRL/AFOSR/IOE (EOARD)

11. SPONSOR/MONITOR'S REPORT NUMBER(S)

AFRL-AFOSR-UK-TR-2014-0027

12. DISTRIBUTION/AVAILABILITY STATEMENT

Distribution A: Approved for public release; distribution is unlimited.

13. SUPPLEMENTARY NOTES

14. ABSTRACT

The first phase of this project focused on the exploitation of the novel high-order regional statistics for Random Finite Set (RFS)-based multi-object filters, estimating the size of the target population, with associated uncertainty, and in any desired region of the surveillance scene. First phase concluded that: (1) Regional statistics are a promising tool for the assessment of situational awareness because they are able to estimate the performance of the multi-object filter in any desired region of the state space; (2) RFS-based multi-object filters, however, have limited use since they do not propagate individual information on targets, but only collective information on the target population (i.e. no tracks are maintained). The second phase explored the construction of a novel filtering solution for multiple-target tracking with the following core requirements in mind: The solution must be derived from a well-defined and well-identified probabilistic framework; It must be compatible with the higher-order regional statistics, and more generally with the available statistical tools for the assessment of RFS-based multi-object filters; It must maintain specific information on identified targets (i.e. tracks). A novel multi-object filtering framework, describing the objects of interest through the concept of stochastic population, has recently been proposed and allows the construction of a novel class of multi-object filters fulfilling the requirements above. This second phase illustrates this multi-object filtering framework on the tracking of multiple targets on simulated orbital scenarios driven from SSA problems. Unlike those derived from the FISST framework, the multi-target detection and tracking algorithms derived from this alternative framework maintain an inherent history of past estimates and past observations for each potential target identified through at least one detection across the scenario. Because the orbital dynamics captured by the Shepperd transition matrix are relatively accurate and close enough to the real dynamics of the targets, the proposed tracking algorithm is able to maintain tracks for targets even when they are long gone from the sensor's field of view, and discriminates new targets from targets re-entering the field of view with good accuracy. Results from this study are illustrated in videos contained in the main report. On a more fundamental level, while the initiation of tracks in SSA problems where sensor observability is limited is a challenging problem in itself that deserves more thorough investigations, the novel probabilistic framework provides grounds for a natural extension of the tracking algorithm in order to accommodate for sensors with limited observability.

15. SUBJECT TERMS

EOARD, multi-object filtering, Finite Set Statistics Theory, AEGIS, Probability Hypothesis Density, object tracking

16. SECURITY CLASSIFICATION OF:			17. LIMITATION OF ABSTRACT	18, NUMBER OF PAGES	19a. NAME OF RESPONSIBLE PERSON
a. REPORT	b. ABSTRACT	c. THIS PAGE			Kevin Bollino
UNCLAS	UNCLAS	UNCLAS	SAR	17	19b. TELEPHONE NUMBER *(Include area code)* +44 (0)1895 616163

Multi-object filtering for space situational awareness

Daniel Clark, Associate Professor, Heriot-Watt University.
Emmanuel Delande, Research Associate, Heriot-Watt University.
Carolin Früh, TEES Assistant Research Scientist, Texas A&M Unversity,
Visiting Postdoctoral Assistant, Heriot-Watt University

1 Background

There is increasing concern about the hazards of space debris and potential harm for satellites and its impact on future space exploration activities. Space debris has largely been caused by waste products from human activity [1]. There are now several hundred thousand objects that have the potential to cause significant damage.

The most recent examples of debris producing events are the 2007 Chinese anti satellite weapon test, in which a decommissioned weather satellite was intentionally destroyed, and the 2009 Iridium/Kosmos collision, in which there was an accidental collision between an active and a defunct communications satellite. In both scenarios many more hundreds of thousands of debris pieces were created.

It is becoming increasingly important to be able to accurately model these events and track the resulting debris in order to avoid harm to expensive space-related infrastructure. Specific concerns related to monitoring of space debris are:

- Tracking the trajectories of individual targets;
- Estimation of the number of objects in the surveillance region with an associated level of uncertainty;
- Detection and estimation of objects arising from target collision.

The Finite Set Statistics (FISST) methodology [20] provides a unified theoretical framework for the study of detection, identification and tracking problems. For this reason, the approximate but efficient Probability Hypothesis Density (PHD) filter [18] and its subsequent implementations have been the subject of growing interest from the tracking community. Although limited to the exploitation of first-order information on the number of targets across the surveillance space, the PHD filter proved to be an effective alternative to classical track-based approaches by alleviating the specific issues related to track creation and deletion.

Yet the need for an enhanced space situational awareness, fuelled by the increased availability of new high-performance computing resources and the more user-friendly implementation tools in algorithm development languages such as Matlab, has recently shifted the focus of research groups towards the design of more general multi-object filters within the Finite Set Statistics framework. While historical developments led to inexpensive solutions that did not propagate information on individual targets, such as Mahler's PHD and Cardinalized Probability Hypothesis Density (CPHD) [19] filters, recent multi-object filtering solutions propose more advanced structures in order to handle the identification of individual targets. Notably, an Adaptative Entropy-based Gaussian mixture Implementation of the full multi-target Bayes filter was proposed for a unitary then arbitrary but known number of targets in [16, 17], and a multi-object filter incorporating target labelling for individual target detection was proposed in [27].

In the context of space situational awareness, both extremities on the scale of available multi-object filters – from inexpensive and "crude" approximates to more advanced solutions closer to the full multi-object Bayes filter [20] – have their advantages. The PHD and CPHD filters are well-established filters whose implementation is widely available and computationally inexpensive. In addition, they are able to handle multi-target detection and tracking problems with a large number of objects, and could be particularly useful to provide a rough estimate of the situational awareness in a region of the space where the number of object has recently increased and their spatial distribution is largely unknown (for example in the aftermath of a collision). On the other hand, in a portion of space where the apparition of new objects – in the sense that they have never been detected beforehand – is highly improbable, a more advanced filter propagating individual information for each object would be more adapted. The labelled RFS filter [27] seems to provide an appropriate solution, but it was proposed very recently and its implementation appears to be particularly challenging.

Independently to the improvement of multi-object filter capabilities, recent theoretical developments [5, 6] in the multi-object filtering framework were proposed, drawn from the more general point process theory. They led to the construction and the practical extraction of higher-order statistics describing the output of multi-object filters [10]. Notably, the novel regional variance in target number can be exploited to quantify the uncertainty in the estimation of the target number, evaluated in any arbitrary region of the surveillance scene, provided by a given multi-object filter. This novel concept has recently been implemented for the single-sensor PHD and CPHD filters [7, 8].

2 Study overview: motivation and objectives

This short study follows and complements the four-month study delivered as the first phase of the USAF EOARD Grant 13-3030. The first phase focussed mainly on the exploitation of the novel high-order regional statistics for multi-object filters, estimating the size of the target population, with associated uncertainty and in any desired region of the surveillance scene. Available for any multi-object filtering solution derived from the FISST framework [20], it is a valuable tool for a comparison between popular multiple-target tracking filters [10] or, as illustrated in the first phase, for an assessment of their extensions adapted to multi-sensor scenarios. Since the availability of the PHD filter [18] and the growing popularity of the multi-object filtering solutions, the axes of development in multi-object filtering have focussed almost exclusively on solutions estimating the target *population* as a whole without maintaining individual information on specific targets (i.e. *tracks*), such as the PHD [18] or CPHD [19] filters. In consequence, the common multi-object filtering solutions are of limited applicability to space awareness scenarios, where maintaining individual information on targets is often required for classification purposes. To this regard, the study of the first phase concluded in the necessity of developing a novel multi-object filtering solution incorporating individual information, and provided early development leads on that topic.

Following the conclusions of the first phase, we explored the construction of a novel filtering solution for multiple-target tracking with the following core requirements in mind:

1. The solution must be derivated from a well-defined and well-identified probabilistic framework;
2. It must be compatible with the higher-order regional statistics, and more generally with the available statistical tools for the assessment of FISST-based multi-object filters;
3. It must maintain specific information on identified targets (i.e. *tracks*).

The last two points are self-explanatory with regard to the discussion above, but the first requirement deserves more explanation. While traditional tracking approaches such as Multiple Hypothesis Tracking (MHT) [22] and Joint Probabilistic Data Association (JPDA) approaches [4] do produce tracks on individual targets, the resulting tracking algorithms *a*) are based on heuristics (e.g. for the creation of a new track) whose consequences on the tracking performance are difficult to identify and quantify, and *b*) do not propose a probabilistic description of the global target population, necessary to the second requirement stated above.

A novel multi-object filtering framework, describing the object of interest through the concept of stochastic population [9, 13, 14], has recently been proposed and allows the construction of a novel class of multi-object filters fulfilling the requirements above. The aim of this short study is to illustrate this multi-object filtering framework on the tracking of multiple targets on simulated orbital scenarios driven from space situational awareness problems.

Section 3 describes the ISP filter and the motivations behind its construction, while Section 4 describes the construction of the orbital scenarios, and the incorporation of their specific elements in the filtering process. Section 5 illustrates the filter on selected scenarios; finally, Section 6 concludes and discusses a possible extension of the ISP filter for the future incorporation of more realistic sensor models.

3 The multiple-target detection and tracking framework

3.1 Principle: stochastic populations and target distinguishability

The underlying principle of the new filtering framework [9, 13, 14] is to provide means to describe each target in the surveillance scenario with the *right amount of information* (i.e. not too little, but not too much either). The

new filtering framework considers two classes of targets, the *indistinguishable* and the *distinguishable* ones, and maintains a different level of description for a elements of each class.

One of the main strength of the FISST framework [20] is its ability to maintain and update a probabilistic description of the target population across the scenario – very effectively and with a limited computational cost, because it does not require explicit data association between targets and measurements. On the other hand, no information is available on the target level, i.e., the target population is described through *a*) some cardinality function, estimating its size, *b*) a *single* spatial distribution, estimating the localization of *all* the targets. This level of description is adapted to the study of target populations for which neither prior information nor collected data is available for any particular individual; e.g. to describe the spread of debris following the collision of two satellites *before any recorded observation of the event* or, more generally, the arrival of new objects in the surveillance scene. Such a population is thus adequately described by a stochastic population of *indistinguishable* individuals.

Before long, observations of indistinguishable individuals through the sensor system can be expected. Once a potential target has been associated to a particular measurement it can be characterised for the rest of the surveillance scenario, *even after is has left the scene*, by the sequence of measurements it has produced across time. That is, an indistinguishable target becomes *distinguishable* upon its first detection, and information about its probability of presence *and* its (eventual) localization in the scene is maintained through a *track* for the remainder of the scenario. Taken together, these tracks constitute a stochastic population of *distinguishable* individuals.

By ensuring that individual information is maintained, but only for (potential) targets identified through observations they have (allegedly) produced, we believe that a two-level description of the targets has the potential to produce clearer filtering expressions, more easily implementable in efficient algorithms, than recent solutions derived within the FISST framework and incorporating track labelling such as the labelled multi-Bernoulli filter [27].

3.2 Filter derivation: key modelling assumptions

Ouf of the general filtering framework [14], well-identified modelling assumptions must be produced in order to derive practical multi-target tracking algorithms. The algorithm that we developed for a previous study (illustrated in Section 3.3) and that we exploited for the simulation results in Section 5 was designed to be as close as possible to the optimal Bayesian solution, under a few well-identified modelling assumptions that can be summarised as follows:

1. Targets behave independently throughout scenario;
2. Collected observations are independent;
3. At most one observation stem from each target at each time step (if none, the target is *mis-detected*);
4. At most one target stem from each observation at each time step (if none, the observation is a *false alarm*);
5. Targets are immediately detected upon entering the scene.

The first four assumptions are commonly assumed in many tracking applications. The fifth assumption means that, for filtering purposes, a target will be considered as having just entered the scene upon its first detection. In particular, the proposed multi-target tracking algorithm does not maintain information about targets that appear outside of the sensor's field of view, until the moment where they are detected for the first time (see an illustration in Section 5). Although the novel framework will lead to the derivation of alternative solutions with less stringent assumptions in the near future, it is out of the scope of this study.

Broadly speaking, the algorithm exploited in this study propagates as much information as possible under the proviso of the modelling assumptions above, and aims at filling the role of a reference filter for the future assessment of multi-object filters, in particular through the exploitation of the higher-order regional statistics [10].

3.3 Tracking algorithms: context of development

Two solutions have been derived from the multiple-target tracking framework so far, in the context of ground surveillance scenarios with radars. The *Hypothesised multi-object filter for Independent Stochastic Population* (HISP) [13] aimed at proposing a inexpensive solution (i.e. comparable to the PHD filter) to multiple-target tracking problems, but with the availability of individual information on targets propagated through tracks. The *multi-object filter for independent Stochastic Population* (ISP) is a more computationally demanding solution that propagates information on the individual target level (tracks) as well as on the multi-target configuration level (group of tracks), and is more suitable to challenging situations such as targets with close and/or crossing trajectories. The topic of an upcoming submission in a IEEE journal, the latter algorithm was chosen for this study and exploited for the simulation results presented in Section 5.

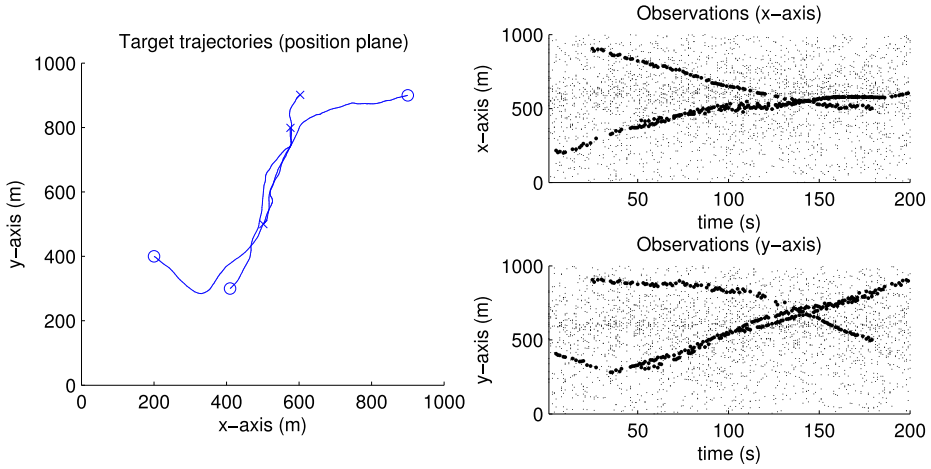

Figure 1: Left: target true trajectories. Circles denote target births, and crosses target deaths. Right: bold dots denote true measurements, and light dots false alarms.

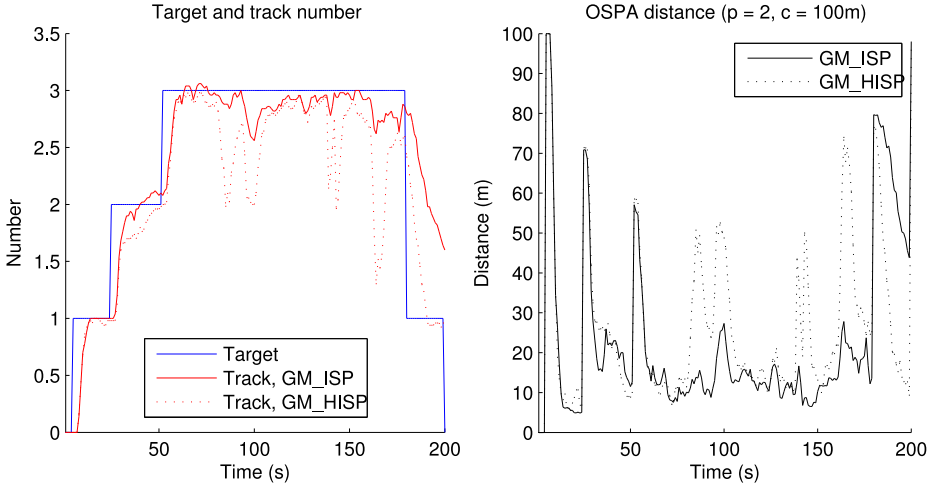

Figure 2: Simulation results (SNR = 9dB, $p_{\text{fa}} = 1e-04$, $p_{\text{d}} = 0.65$).

Figure 1 shows a challenging ground surveillance scenario in which three targets have close trajectories, and are observed by a range-bearing radar with mediocre detection capabilities – false alarm rate is $p_{\text{fa}} = 1e-04$, probability of detection is $p_{\text{d}} = 0.65$. Figure 2 show that both filters maintain a low level of OSPA [23] distance, which suggests a good and steady detection and tracking performance throughout the scenario (with the notable exception of the last time steps, discussed later on in this paragraph). The short spikes in the OSPA distance at the beginning of the scenario suggest that both filters handle the appearance of new targets fairly well. Note that additional spikes in the OSPA distance occur in particularly challenging time steps where targets are crossing.

They are quite noticeable in the case of the HISP filter, which is built on a modelling approximation with limited consequence when targets are isolated, but induces a significant loss in tracking accuracy when targets are getting close to each other in the physical space. On the other hand the drop in tracking performance is very limited in the case of the ISP filter, designed as a reference filter able to handle any situation provided that targets behave independently. The general drop in the tracking performance at the end of the scenario can be explained by the fact that targets disappear suddenly from the scene, while the target behaviour model fed to the filters covers target disappearances upon reaching the boundaries of the surveillance scene. The ISP filter, based on less stringent assumptions than the HISP filter, is more confident in its estimation and less flexible to modelling errors, hence the sharper performance drop occurring when targets are leaving the scene unexpectedly.

4 Modelling of orbital scenarios

4.1 Target state transition

The state transition matrix captures the dynamics of the targets (usually approximately) and is fed to the filter in order to predict the targets' evolution in the Bayesian paradigm. In this study, a simplified model of purely Keplerian dynamics has been implemented for the transition matrix, i.e.

$$\ddot{\mathbf{r}} = -\frac{\mu \mathbf{r}}{r^3}, \tag{1}$$

where $\mathbf{r}$ is the object's position vector in space fixed Earth centred inertial (ECI) frame, μ is the Earth gravitational constant, and $r = |\mathbf{r}|$ is the distance from the object to the centre of the ECI frame. At any time t, the dynamics of a target is described in ECI frame by *a*) its position coordinates $\mathbf{r}(t)$ (three variables), and *b*) its velocity coordinates $\mathbf{v}(t)$ (three variables). The state transition matrix $\Phi(t, t_0)$, describing the evolution from coordinates $\mathbf{r}_0 = \mathbf{r}(t_0), \mathbf{v}_0 = \mathbf{v}(t_0)$ to coordinates $\mathbf{r} = \mathbf{r}(t), \mathbf{v} = \mathbf{v}(t)$, can be written as follows:

$$\begin{pmatrix} \mathbf{r} \\ \mathbf{v} \end{pmatrix} = \Phi(t, t_0) \begin{pmatrix} \mathbf{r}_0 \\ \mathbf{v}_0 \end{pmatrix}, \qquad \Phi(t, t_0) = \begin{pmatrix} \frac{\mathbf{r}}{\mathbf{r}_0} & \frac{\mathbf{r}}{\mathbf{v}_0} \\ \frac{\mathbf{v}}{\mathbf{r}_0} & \frac{\mathbf{v}}{\mathbf{v}_0} \end{pmatrix}. \tag{2}$$

Utilizing the universal variables of Goodyear, the implementation of Shepperd has been chosen, for the computational efficient determination of the transition matrix [12, 24]:

$$\Phi_{11} = f\mathbf{I} + \begin{pmatrix} \mathbf{r} & \mathbf{v} \end{pmatrix} \begin{pmatrix} M_{21} & M_{22} \\ M_{31} & M_{32} \end{pmatrix} \begin{pmatrix} \mathbf{r}_0 \\ \mathbf{v}_0 \end{pmatrix}, \tag{3}$$

$$\Phi_{12} = g\mathbf{I} + \begin{pmatrix} \mathbf{r} & \mathbf{v} \end{pmatrix} \begin{pmatrix} M_{22} & M_{23} \\ M_{32} & M_{33} \end{pmatrix} \begin{pmatrix} \mathbf{r}_0 \\ \mathbf{v}_0 \end{pmatrix}, \tag{4}$$

$$\Phi_{21} = f\mathbf{I} - \begin{pmatrix} \mathbf{r} & \mathbf{v} \end{pmatrix} \begin{pmatrix} M_{11} & M_{12} \\ M_{21} & M_{22} \end{pmatrix}_{v} ideo \begin{pmatrix} \mathbf{r}_0 \\ \mathbf{v}_0 \end{pmatrix}, \tag{5}$$

$$\Phi_{22} = g\mathbf{I} - \begin{pmatrix} \mathbf{r} & \mathbf{v} \end{pmatrix} \begin{pmatrix} M_{12} & M_{13} \\ M_{22} & M_{23} \end{pmatrix} \begin{pmatrix} \mathbf{r}_0 \\ \mathbf{v}_0 \end{pmatrix}, \tag{6}$$

where f, g are the well known functions:

$$\mathbf{r} = \mathbf{r}_0 f + \mathbf{v}_0 g, \qquad \mathbf{v} = \mathbf{r}_0 \dot{f} + \mathbf{v}_0 \dot{g} \tag{7}$$

that can be determined according to [24]. The matrix $\mathbf{M}$ can be determined as linear combinations of the f, g functions and its derivatives, together with the orbital parameters. Kepler's equation is solved via Newton Raphson's iteration.

4.2 Reference trajectories

The targets in the scenario follow reference trajectories, unknown to the filter since it is only fed with the approximate transition matrix. The reference trajectories were computed according to the following model:

$$\ddot{\mathbf{r}} = -\mu \nabla V(\mathbf{r}) - G \sum_{k=1,2} M_k \left[\frac{\mathbf{r} - \mathbf{r}_k}{|\mathbf{r} - \mathbf{r}_k|^3} + \frac{\mathbf{r}_k}{r_k^3} \right] + \sum_l \mathbf{a}_l \tag{8}$$

where V is the Earth's gravitational potential. For its representation, the formulation of Pines [21] was chosen, and transformed in the Earth centred space fixed coordinate system. The third body gravitational perturbations of the sun and moon ($k = 1, 2$) with the states $\mathbf{r}_k$ have also been taken into account. Finally, $\sum \mathbf{a}$ is the sum over all non-gravitational accelerations acting on the satellite. These latter perturbations can include accelerations due to direct solar radiation pressure (SRP) and, hence, the attitude dependence finds its way into the equations of motion. If attitude dynamics are modelled, these must be included in the integration of the equations of motion. As non-gravitational perturbations, solar radiation pressure in the canon-ball model has been taken into account, leading to the following acceleration:

$$\mathbf{a}_{rad} = -F_p \cdot C \frac{A}{m} \frac{E}{c} \frac{A_{\text{Earth}}}{|\mathbf{r} - \mathbf{r}_{\text{Sun}}|} \mathbf{e}_{\text{satSun}} \tag{9}$$

where C is the reflection coefficient, which is assumed to be one, A is the area of the object, m is its mass, E is the solar constant, c is the speed of light, A_{Earth} is the astronomical unit, $\mathbf{r}_{\text{Sun}}$ is the ECI sun position, and $\mathbf{e}_{\text{satSun}}$ is the unit vector from the satellite position to the sun. F_p, is the scaling parameter accounting for the Earth shadow. Earth shadow passages are simulated with a dual cone model mixture. The dual cone model assumes an extended sun, but ignores limb darkening, which leads to the following set of equations, named Baker functions [2]:

$$F_p = 1 - \frac{(\gamma/\tau)^2(\delta - \sin(2\delta)/2) + (\beta - \sin(2\beta)/2)}{\pi}, \tag{10}$$

with:

$$\begin{aligned}
\gamma &= \arcsin(a_{\text{Earth}}/r), \\
\tau &= \arcsin(a_{\text{Sun}}/r_{\text{satSun}}), \\
\epsilon &= \arccos(\mathbf{e}_{\text{satSun}} \cdot \mathbf{e}) \begin{cases} \epsilon > \gamma + \tau & \text{whole sun disc visible} \\ \tau + \epsilon < \gamma & \text{no sun disc is visible} \\ \text{otherwise} & \text{fraction of the sun disc visible} \end{cases}, \\
s &= (\tau + \gamma + \epsilon)/2, \\
k &= \sqrt{(s(s-\tau)(s-\gamma)(s-\epsilon))}, \\
\sin(\delta) &= \frac{2k}{\epsilon\gamma}, \\
\sin(\beta) = \sin(\delta) &= \frac{2k}{\epsilon\tau}, \\
\cos(\delta) &= \frac{\epsilon^2 + \gamma^2 - \tau^2}{2\epsilon\gamma}, \\
\cos(\beta) &= \frac{\epsilon^2 + \gamma^2 - \gamma^2}{2\epsilon\tau},
\end{aligned}$$

where a_{Earth} is the mean Earth radius and $\mathbf{e}$ is the ECI satellite direction. In order to overcome known deficiencies with the simple dual cone model, a physical model in a weighted sum of the Baker functions according to Hujsak [15] has been chosen:

$$\tilde{F}_p = \sum_{i=1}^{5} w_i F_p(\tilde{r}_i), \tag{11}$$

with:

$$\begin{aligned}
\{\tilde{r}_i\} &= \{a_{\text{Earth}} + 48, a_{\text{Earth}} + 32, a_{\text{Earth}} + 16, a_{\text{Earth}}, a_{\text{Earth}} - 40\}, \\
\{w_i\} &= \{2/9, 2/9, 2/9, 2/9, 1/9\}.
\end{aligned}$$

4.3 Multiple target scenario

The multiple target scenario was created by producing several Keplerian orbits with an Earth gravity field of degree and order 12, third body perturbations and solar radiation pressure taken into account (see Sections 4.1 and 4.2). The initial orbital elements and area to mass ratios are listed in Table 1. The start epoch is 53159.5 MJD, the propagation duration is one day.

Target no.	a (km)	e	i (°)	Ω (°)	ω (°)	ν (°)	AMR (m^2/kg)
1	42164.0	0.01	13.0	60.0	351.0	84.0	0.02
2	42164.0	0.01	170.0	50.0	30.0	20.0	0.60
3	42164.0	0.8	11.3	60.0	351.0	80.0	0.02
4	8882.0	0.1	12.0	61.0	354.0	83.0	0.02
5	6882.0	0.1	60.0	61.0	354.0	83.0	0.5

Table 1: Semi-major axis, eccentricity, inclination, right ascension of the ascending node, argument of perigee, true anomaly and area-to-mass ratio.

4.4 Sensor

In order to illustrate the multi-target scenario with the orbital trajectories described above, we modelled a sensor, which is starting in the fixed zenith direction throughout the scenario and is placed on the Earth equator: the sensor's field of view is thus in rotation in the space fixed Earth centred (ECI) reference frame. The sensor's field of view defines a radar-like sensing region of about 45×10^6 m deep, 15° wide, in Earth fixed coordinates. Due to its equatorial position it is hence covering the inclinations from $-45°$ to 45°.

This study aims at illustrating the ability of the filter to maintain initiated tracks across time, when the field of view is limited, a common issue in space situational awareness considering the vastness of space and the tremendous amount of single objects, that needs to be covered with a limited amount of sensing capabilities. Another specific issue that is not addressed in the current study is the track initialization or first orbit determination in observation of an incomplete state. Realistic sensors, such as radar or optical measurements, are only able to provide a subset of the whole state in a single measurement. First orbit determination methods range from classical methods, such as Gauss, Herrick-Gibbs, Gooding [3, 26] to more recent developments, such as admissible regions approach [11, 25]. Currently, this aspect has been neglected, assuming a full physical space (e.g. angular velocities and/or radial velocity in spherical coordinates not measured) would be available in the single measurement of our radar-like sensor. To extend the work to realistic sensing capabilities is the next and most pressing development step in the filter development, see Section 6.

The characteristics of the sensor are summarized in Table 2. In addition, the probability of false alarm per cell is set at $p_{\text{fa}} = 5.10^{-15}$, inducing an average of two false alarms per scan, and the probability of detection is set at $p_{\text{d}} = 0.8$.

Table 2: Sensor model: cell resolution and noise profile

cell resolution						noise (standard deviation)					
r	θ	φ	$\dot{r}$	$\dot{\theta}$	$\dot{\varphi}$	r	θ	φ	$\dot{r}$	$\dot{\theta}$	$\dot{\varphi}$
1000 m	1°	1°	100 m s^{-1}	1° s^{-1}	1° s^{-1}	1000 m	1°	1°	100 m s^{-1}	1° s^{-1}	1° s^{-1}

Figure 3 below depicts the observations produced by the sensor over the whole simulation on the simulated orbital scenario with the five targets described in Section 4.3. The left part illustrates the moving targets on the reference trajectories (marked by blue paths), the grey volume depicting the current sensor's field of view. The right part illustrates the observations produced by the sensor, cumulated over the whole duration of the scenario (one day). True measurements (resp. false alarms) are depicted by dots (resp. crosses).

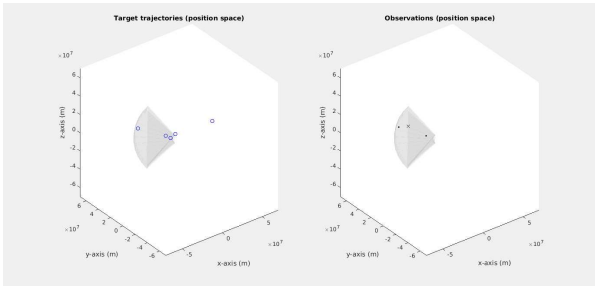

(a) Observations, $t = 1$

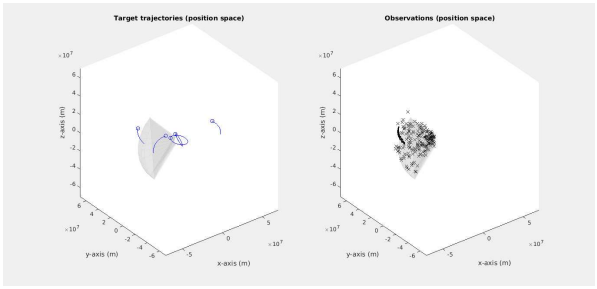

(b) Observations, $t = 97$

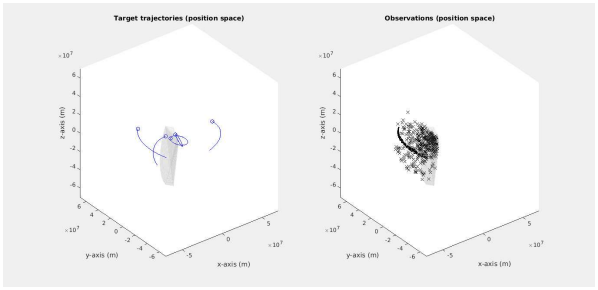

(c) Observations, $t = 193$

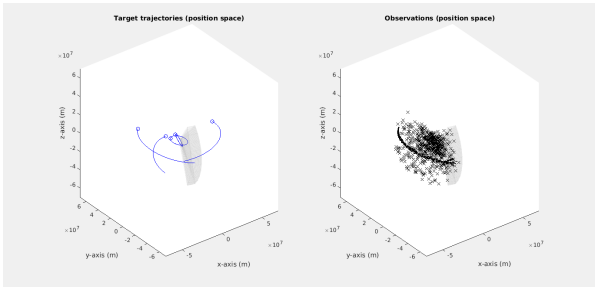

(d) Observations, $t = 289$

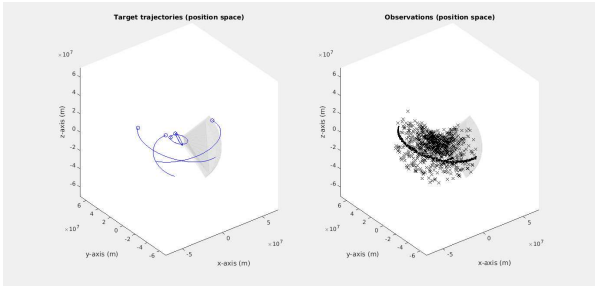

(e) Observations, $t = 385$

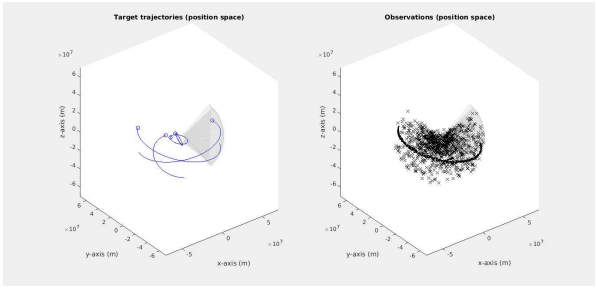

(f) Observations, $t = 481$

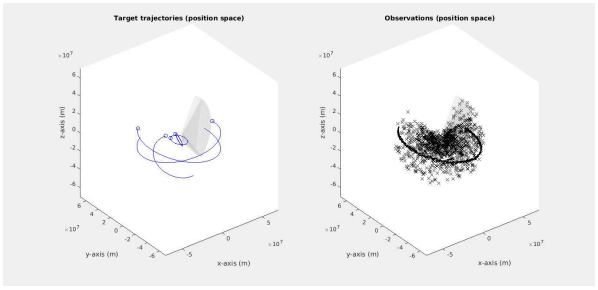

(g) Observations, $t = 577$

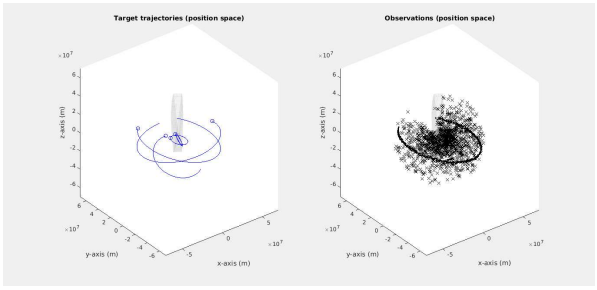

(h) Observations, $t = 673$

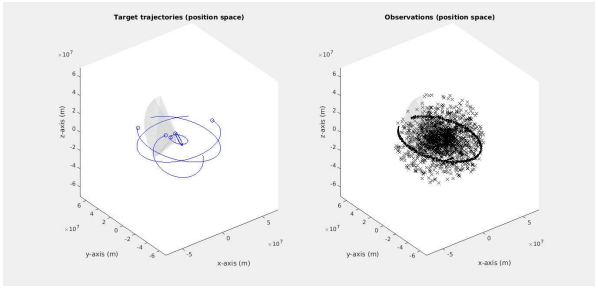

(i) Observations, $t = 769$

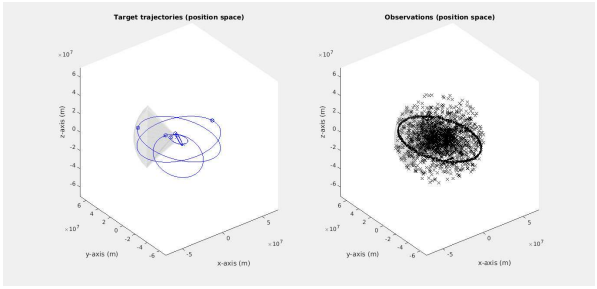

(j) Observations, $t = 864$

Figure 3: Observations across the scenario. True trajectories are depicted in blue on the left-hand side figure. True observations (resp. false alarms) are depicted with bold dots (resp. crosses) on the right-hand side figure.

5 Simulation results

We illustrate the ISP filter on the beginning of the one-day-long scenario described in Sections 4.3 and 4.4 (see Figure 3 above). During this 8 h20 min-long period, the five targets evolve on five different orbits as described in Table 1. Target 1 is on a geostationary orbit, and situated at the vertical of the sensor; therefore, it is susceptible of being detected throughout the whole duration of the scenario. Target 2 is on a retrograde geostationary orbit and only meets the sensor's field of view once throughout the selected time period. Target 3 is on a geostationary transfer orbit, and meets the field of view only once during the scenario as well. Target 4 is on a low Earth orbit, and in the same plane as target 1; rotating much faster than the sensor, it meets the field of view several times during the selected time period. Finally, target 5 is on a highly inclined low Earth orbit; while it rotates faster than the field of view, the initial position of the sensor is such that the target does not meet the field of view before a long time.

Figures 4 and 5 below depict the filter output over the selected time period. A green diamond indicates the current position of some track, i.e., the estimated position of a (potential) target identified by the filter. The green ellipsoid illustrates the uncertainty of the filter in the estimation of the position. Finally, the sequence of past positions of a track is illustrated by a green line. Note that only tracks with high credibility are displayed. More precisely, the filter may produce tentative tracks if a stream of measurements is coherent enough to denote the birth of a new object, but the probabilistic framework behind the ISP filter allows the operator to assess the likelihood of any track, for displaying purposes, through a well-defined *probability of existence*.

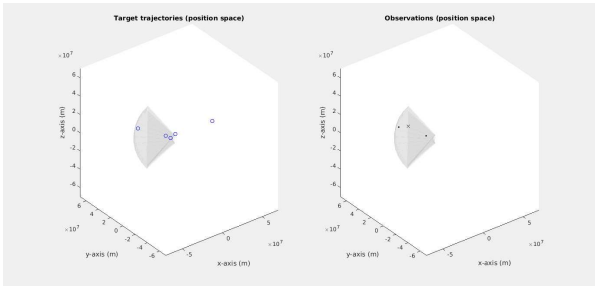

(a) Filter output, $t = 1$

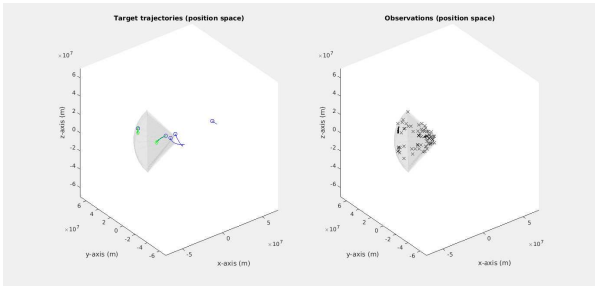

(b) Filter output, $t = 34$

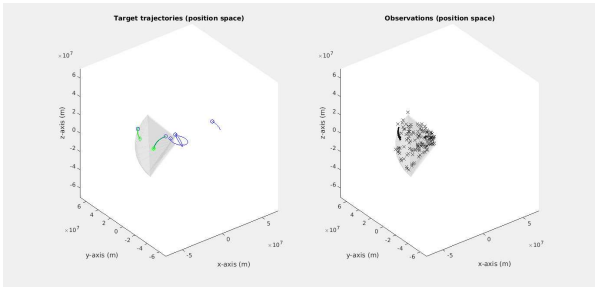

(c) Filter output, $t = 67$

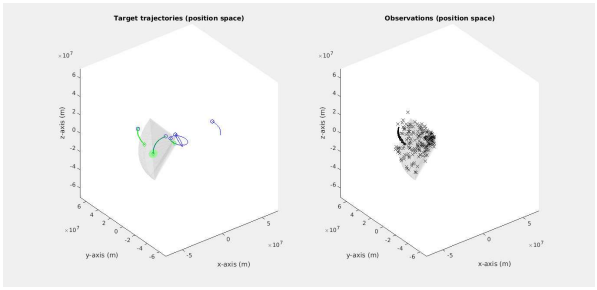

(d) Filter output, $t = 100$

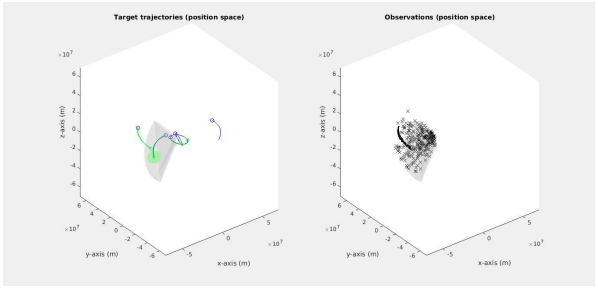

(e) Filter output, $t = 133$

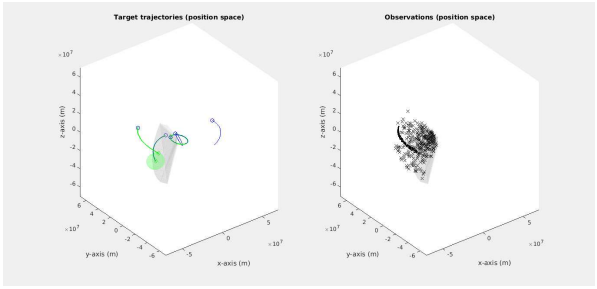

(f) Filter output, $t = 166$

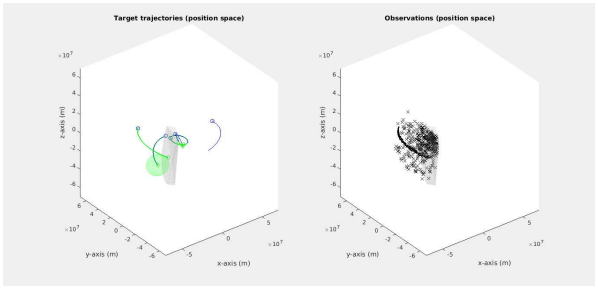

(g) Filter output, $t = 199$

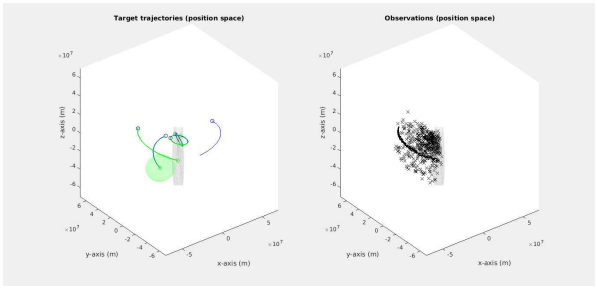

(h) Filter output, $t = 232$

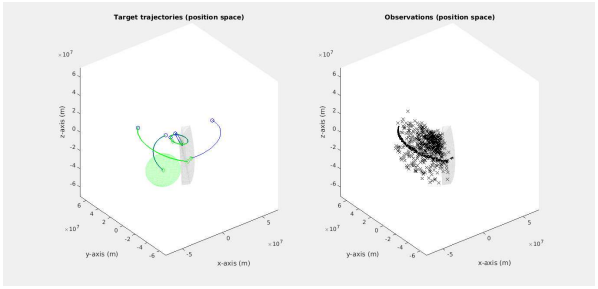

(i) Filter output, $t = 265$

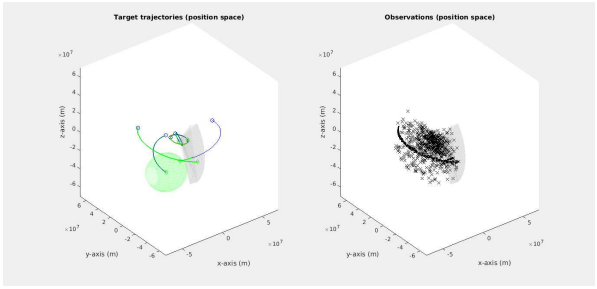

(j) Filter output, $t = 300$

Figure 4: Filter output across the selected period of the scenario. Estimated trajectories are depicted in green on the left-hand side figure. The green ellipsoids depict the uncertainty on the targets' estimated position.

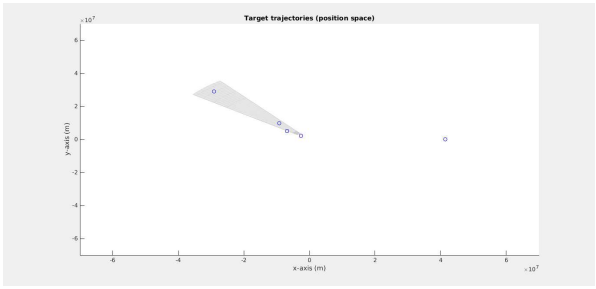

(a) Filter output (detail), $t = 1$

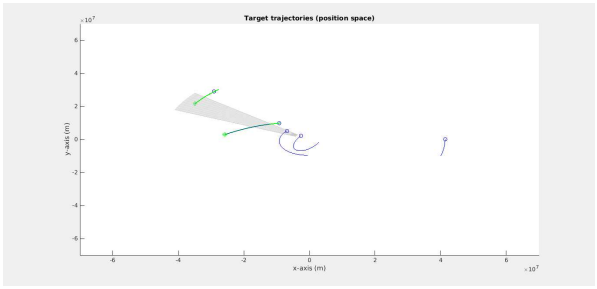

(b) Filter output (detail), $t = 34$

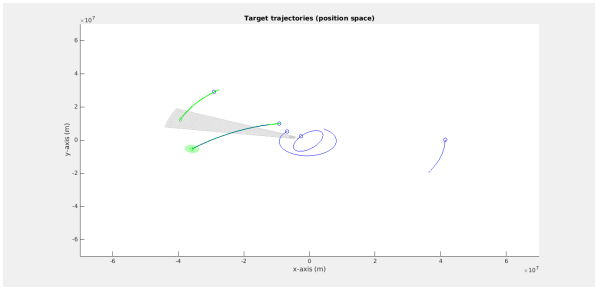

(c) Filter output (detail), $t = 67$

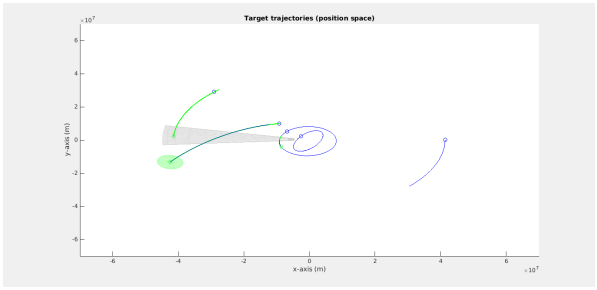

(d) Filter output (detail), $t = 100$

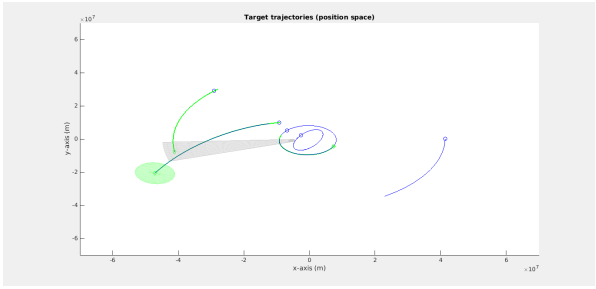

(e) Filter output (detail), $t = 133$

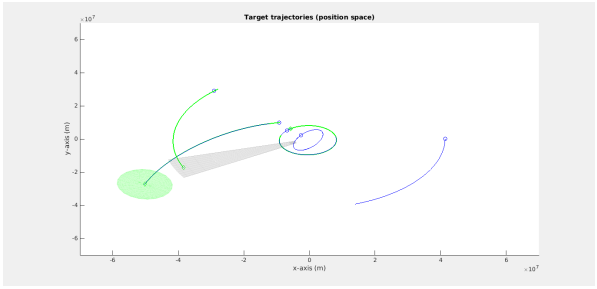

(f) Filter output (detail), $t = 166$

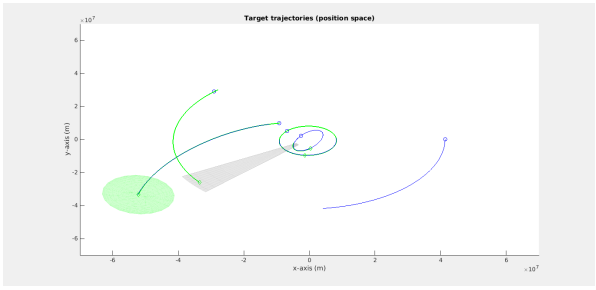

(g) Filter output (detail), $t = 199$

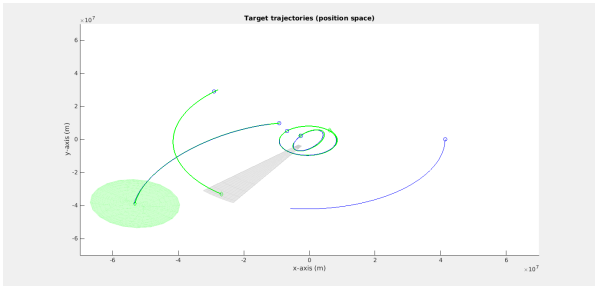

(h) Filter output (detail), $t = 232$

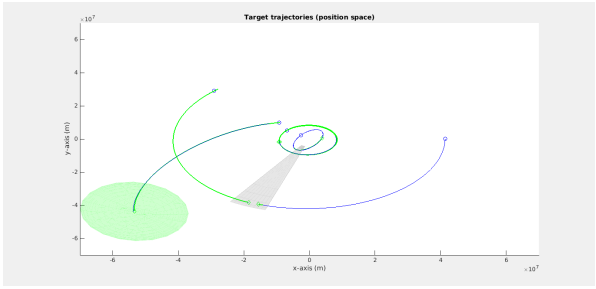

(i) Filter output (detail), $t = 265$

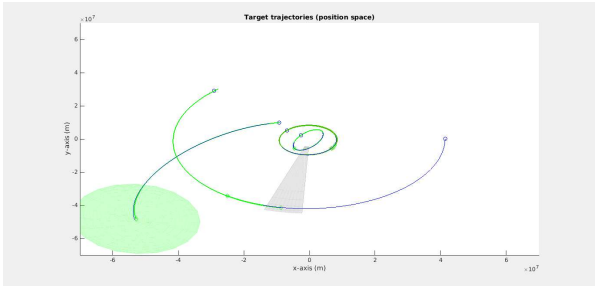

(j) Filter output (detail), $t = 300$

Figure 5: Filter output across the selected period of the scenario (detail). Estimated trajectories are depicted in green on the left-hand side figure. The green ellipsoids depict the uncertainty on the targets' estimated position.

Unsurprisingly, target 1 is detected almost right away by the filter, and a track with low uncertainty is maintained throughout the whole selected period. Target 2 is largely ignored by the filter since it does not meet the field of view of the sensor, until the very end of the selected period where a track is correctly initiated and maintained by the filter. Target 3 presents a different case: its trajectory crosses the field of view early in the period and the filter correctly initiates a track, but it then recedes from the Earth and never crosses the field of view ever again. The probability of survival fed to the filter being particularly high ($1 - 10^6$), the filter maintains the track throughout the selected period, albeit with a growing uncertainty on the target's position. Note that the error between the estimated position and the true position of target 3 increases gradually over time as soon as new observations are unavailable to correct the filter's imperfect prediction through the Shepperd transition matrix. Note that the probability of presence of the track, i.e. the probability that the associated target is still present in the scene, is gradually reduced by the filter since no new observation can confirm the continuous presence of the object in space. However, due to very high probability of survival in the model fed to the filter, this decrease is marginal over the duration of the selected time period.

The tracking of targets 4 and 5 present similar issues that will be resolved in future developments of the filter. While target 4 is rapidly identified by the filter and its corresponding track successfully maintained by the filter for two rotations around the Earth, a "fake" track is created by the filter at the third passage and clearly noticeable at the end of the scenario. The cause of this discrepancy is likely to be found in the border effect of the sensor's field of view, not explicitly modelled in the current implementation of the ISP filter. The filter does not consider a track a valid candidate for data association as long as its *mean position* (depicted by the green diamond in the figures) does not fall within the field of view, *regardless of the size of the uncertainty* (depicted by the green ellipsoid in the figures). Thus, even if a track is correct in the sense that the position of the underlying target lies within the ellipsoid, the filter will fail to associate the track with the measurements produced by the target if the latter lies in the sensor's field of view *as well*. In consequence, the filter will create a *new* track from the stream of coherent measurements, for lack of a better option in data association. As soon as the "genuine" track enters the field of view as well, the two tracks compete for the same measurements: the filter will gradually decrease the probability of presence of one of the two tracks – as seen, for target 4, by the bright green of one of the two tracks turning into a darker green in the last step of the selected period – which will eventually be discarded by the filter – as seen, for target 5, when it crosses the field of view for the second time.

A first solution to explore to tackle this issue would be to incorporate the uncertainty of the track's position in the evaluation of the distance between the track and the sensor's field of view – e.g. using the Mahalanobis distance rather than the Euclidian distance, but this is out of the scope of this study.

6 Conclusion and further work

The main objective of this short study was to illustrate the adaptability of a recently developed multi-object framework to orbital scenarios in space situational awareness problems. Unlike those derived from the FISST framework, the multi-target detection and tracking algorithms derived from this alternative framework maintain an inherent history of past estimates and past observations for each potential target identified through at least one detection across the scenario. Because the orbital dynamics captured by the Shepperd transition matrix are relatively accurate and close enough to the real dynamics of the targets, the proposed tracking algorithm is able to maintain tracks for targets even when they are long gone from the sensor's field of view, and discriminates new targets from targets re-entering the field of view with good accuracy.

Two axes of future development have been identified. First, the analysis of the simulated scenario suggests that a better modelling of the border effect of the sensor's field of view would prevent the creation of an undesirable track that sometimes occurs when low Earth orbit targets are re-entering the field of view. On a more fundamental level, the initiation of tracks in space situational awareness problems where sensor observability is limited is a challenging problem in itself that deserves more thorough investigations. However, the probabilistic framework upon which the proposed tracking algorithm is based provides grounds for a natural extension of the tracking abilities in order to accommodate for sensors with limited observability. While the localization of each track in the physical space is currently described by a single probability distribution, it would be straightforward to extend the filtering equations to more general solution where each track is described by a weighted sum of probability distributions, where the relative importance of each distribution is updated each time a new observation is associated to the

track. The probability distributions could then be initiated in order to cover the unobserved dimensions of the state space through several well-chosen orbits. Since the data association mechanism is independent of the nature of the spatial distribution maintained for each track, the complexity of the tracking would scale linearly with the number of probability distributions maintained for each track. One distribution being likely to become preponderant in the weighted sum once a track has been assigned to enough observations, distributions with negligible weight could be discarded along the update process in order to reduce the computational cost of the tracking process without significant performance loss.

References

[1] M. Ansdell. Active Space Debris Removal: Needs, Implications, and Recommendations for Today's Geopolitical Environment. Technical report, George Washington University, November 2010.

[2] R. M. L. Baker. *Astrodynamics: Applications and Advanced Topics*. Academic Press Inc., 1967.

[3] R. H. Battin. *An introduction to the mathematics and methods of astrodynamics*. AIAA education series. American Institute of Aeronautics and Astronautics, Reston, VA, 1999.

[4] W. D. Blair and Y. Bar-Shalom, editors. *Multitarget-Multisensor Tracking: Applications and Advances (Volume III)*. Artech House, 2000.

[5] D. E. Clark and J. Houssineau. Faà di Bruno's formula for Gâteaux differentials and interacting stochastic population processes. 2012. arXiv:1202.0264v4.

[6] D. E. Clark and J. Houssineau. Faà di Bruno's formula and spatial cluster modelling. *Spatial Statistics*, 2013.

[7] E. Delande, J. Houssineau, and D. E. Clark. Localised variance in target number for the Cardinalized Hypothesis Density Filter. In *Information Fusion, Proceedings of the 16th International Conference on*, July 2013.

[8] E. Delande, J. Houssineau, and D. E. Clark. PHD filtering with localised target number variance. In *Signal Processing, Sensor Fusion, and Target Recognition XXII, Proceedings of SPIE*, page 87450E, April 2013.

[9] E. Delande, J. Houssineau, and D. E. Clark. Performance metric in closed-loop sensor management for stochastic populations. 2014. accepted.

[10] E. Delande, M. Üney, J. Houssineau, and D. E. Clark. Regional variance for multi-object filtering. *Signal Processing, IEEE Transactions on*, 2013. accepted (arXiv:1310.2873).

[11] D. Farnocchia, G. Tommei, A. Milani, and A. Rossi. Innovative methods of correlation and orbit determination for space debris. *Celestial Mechanics and Dynamical Astronomy*, 107(1-2):169–185, 2010.

[12] W. H. Goodyear. Completely general closed-form solution for coordinates and partial derivative of the two-body problem. *Astronomical Journal*, 70(3):189 – 192, 1965.

[13] J. Houssineau and D. E. Clark. Representation and estimation of stochastic populations. Technical report, Heriot Watt University, 2014.

[14] J. Houssineau, P. Del Moral, and D. E. Clark. General multi-object filtering and association measure. In *Computational Advances in Multi-Sensor Adaptive Processing (CAMSAP), 2013 IEEE International Workshop on*, 2013.

[15] R. S. Hujsak. Solar Pressure. In *Proceedings of Artificial Satellite theory Workshop, USNO*, pages 54 – 72, nov 1993.

[16] I. I. Hussein, K. J. DeMars, C. Früh, R. S. Erwin, and M. K. Jah. An AEGIS-FISST integrated detection and tracking approach to Space Situational Awareness. In *Information Fusion, Proceedings of the 15th International Conference on*, pages 2065–2072, July 2012.

[17] I. I. Hussein, K. J. DeMars, C. Früh, M. K. Jah, and R. S. Erwin. An AEGIS-FISST Algorithm for Multiple Object Tracking in Space Situational Awareness. In *AIAA Guidance, Navigation, and Control Conference 2012*, August 2012.

[18] R. P. S. Mahler. Multitarget Bayes Filtering via First-Order Multitarget Moments. *Aerospace and Electronic Systems, IEEE Transactions on*, 39(4):1152–1178, October 2003.

[19] R. P. S. Mahler. PHD Filters of Higher Order in Target Number. *Aerospace and Electronic Systems, IEEE Transactions on*, 43(4):1523–1543, October 2007.

[20] R. P. S. Mahler. *Statistical Multisource-Multitarget Information Fusion*. Artech House, 2007.

[21] S. Pines. Uniform Representation of the Gravitational Potential and its Derivatives. *AIAA Journal*, 11(11):1508 – 1511, 1973.

[22] D. Reid. An Algorithm for Tracking Multiple Targets. *Automatic Control, IEEE Transactions on*, 24(6):843–854, December 1979.

[23] D. Schuhmacher, B.-N. Vo, and B.-T. Vo. A Consistent Metric for Performance Evaluation of Multi-object filters. *Signal Processing, IEEE Transactions on*, 56(8):3447–3457, August 2008.

[24] S. W. Shepperd. Universal Keplerian state transition matrix. *Celestial Mechanics*, 35:129 – 144, 1985.

[25] G. Tommei, A. Milani, and A. Rossi. Orbit determination of space debris: admissible regions. *Celestial Mechanics and Dynamical Astronomy*, 97(4):289–304, 2007.

[26] D. Vallado and W. McCain. *Fundamentals of Astrodynamics and Applications*. Microcosm Press, El Segundo, California, 2001. ISBN 0-7923-6903-3.

[27] B.-T. Vo and B.-N. Vo. Labeled Random Finite Sets and Multi-Object Conjuguate Priors. *Signal Processing, IEEE Transactions on*, 61:3460 – 3475, jul 2013.